

Large-scale production and purification of functional recombinant bovine rhodopsin with the use of the baculovirus expression system

Corné H. W. KLAASSEN, Petra H. M. BOVEE-GEURTS, Godelieve L. J. DECALUWÉ and Willem J. DEGRIP¹

Department of Biochemistry, Institute of Cellular Signalling, University of Nijmegen, PO Box 9101, NL-6500 HB Nijmegen, The Netherlands

Here we describe a generic procedure for the expression and purification of milligram quantities of functional recombinant eukaryotic integral membrane proteins, exemplified by hexahistidine-tagged bovine rhodopsin. These quantities were obtained with the recombinant baculovirus/Sf9 insect cell-based expression system in large-scale bioreactor cultures with the use of a serum-free and protein-free growth medium. After optimization procedures, expression levels up to 4 mg/l were established. The recombinant rhodopsin could be purified with high overall yield by using immobilized-metal-affinity chromatography on Ni²⁺-agarose. After reconstitution into a native lipid environment, the purified protein was functionally indistinguishable

from native rhodopsin with regard to the following parameters: spectral absorbance band, structural changes after photoactivation, and G-protein activation. The procedures developed can be adapted to other membrane proteins. The ability to produce and purify tens of milligrams of functional recombinant eukaryotic membrane protein meets the ever-increasing demand of material necessary to perform detailed biochemical and structural biophysical studies that are essential in unravelling their working mechanism at a molecular level.

Key words: G-protein-coupled receptor, His-tag, bioreactor, multiplicity of infection, membrane protein.

INTRODUCTION

Rhodopsin is the photoreceptor pigment from the rod cells of the vertebrate retina that allows vision under dim light conditions. This integral membrane protein contains seven transmembrane-spanning domains and belongs to the large family of G-protein-coupled receptors [1]. Members of this family of receptors are widespread in many regulatory functions throughout the vertebrate body. Rhodopsin is probably the only member of this family that can be purified in reasonable quantities from a natural abundant source and has served as a model for this family of receptor proteins for many years. Apart from studies on the native protein, the ability to study rhodopsin mutants produced as recombinant proteins has been indispensable in increasing our insight into the structure and molecular mechanism of action of this membrane receptor protein [2–6]. However, the availability of recombinant material still poses an important limitation. Many techniques for the study of rhodopsin and other receptors [such as UV/visible, fluorescence, ESR and Fourier-transform infrared (FTIR) spectroscopies, G-protein activation and signal pathway assays] require small or only moderate amounts of material. However, crystallization attempts and powerful biophysical techniques, such as Raman spectroscopy and time-resolved UV/visible or FTIR spectroscopy to study ultrafast kinetics and structural changes, or solid-state NMR spectroscopy to determine structural constraints at high resolution, require large amounts of material (up to tens of milligrams) [7,8]. So far, the availability of only limited amounts of recombinant protein has been the major limitation in applying these techniques. Here we demonstrate that we now are able to overcome this limitation. Our approach is based on the recombinant baculovirus expression system in combination with insect cells, because this system is relatively inexpensive and easy to handle. Furthermore, the amount of functional rhodopsin that can be produced with this system exceeds that for any other

expression system used so far [4,9–11]. We optimized a number of key parameters that determine the volumetric yield of recombinant protein and scaled up our culture levels. Here we show that we are able to produce 30–40 mg of rhodopsin in a single 10 litre bioreactor run in suspension culture. Combined with the ability to purify and reconstitute the protein in a native lipid environment with high overall recovery, this will pave the way for high-resolution biophysical studies that are required in unravelling the molecular mechanism of action of this fascinating membrane receptor protein.

EXPERIMENTAL

Detergents

Dodecylmaltose (DOM) and nonylglucose (NG) were from Anatrace (Maumee, OH, U.S.A.) and CHAPS was from Sigma (St. Louis, MO, U.S.A.).

Cell culture and viruses

Sf9 cells (ATCC CRL-1711) were grown and infected in suspension culture in serum-free and protein-free Insect-Xpress medium (BioWhittaker, Walkersville, MD, U.S.A.) to which penicillin and streptomycin (both from Gibco-BRL, Breda, The Netherlands) were added, to 5 i.u./ml and 5 µg/ml respectively. Small-scale cultures (100 ml) were grown in spinner flasks (Bellco, Vineland, NY, U.S.A.). Large-scale cultures were grown in a 7-litre bioreactor (working volume 5 litres) or a 15-litre bioreactor (working volume 10 litres) from Applikon (Schiedam, the Netherlands) under the following culture conditions: temperature 27 °C, partial oxygen pressure 50%, overlay aeration (air) 0.1 vol./min per vol. (v/vm), sparger (O₂) max. 0.005 v/vm (computer-controlled), impeller (marine) 80 rev./min. Total cell counts were made with a haemocytometer; an experimental error of ± 10%

Abbreviations used: DOM, dodecylmaltose; FTIR, Fourier-transform infrared; GTP[S], guanosine 5'-[γ-thio]triphosphate; MOI, multiplicity of infection; NG, nonylglucose; NTA, nitrilotriacetic acid; v/vm, vol./min per vol.

¹ To whom correspondence should be addressed (e-mail wdegrip@baserv.uci.kun.nl).

has therefore to be accounted for. Cells were infected with a recombinant baculovirus carrying the coding sequence for a C-terminally hexahistidine-tagged opsin [12] under the conditions as indicated in the text.

Regeneration of rhodopsin

Infected *Spodoptera frugiperda* (Sf9) cells were collected by centrifugation for 5 min at 3000 *g* (4 °C). The pellet was resuspended at a density of 10⁸ cells/ml in 7 mM Pipes/Na⁺, pH 6.5, containing 10 mM EDTA, 5 mM dithioerythritol and 5 μM leupeptin. The cells were homogenized with six strokes at 150 rpm in a Potter–Elvehjem tube at 4 °C. The homogenate was centrifuged for 20 min at 40 000 *g* (4 °C) to collect the membranes. The pellet was resuspended in half the original volume of 20 mM Pipes/Na⁺, pH 6.5, containing 130 mM NaCl, 10 mM KCl, 3 mM MgCl₂, 2 mM CaCl₂, 0.1 mM EDTA, 5 μM leupeptin and 0.5 mM DOM. All subsequent manipulations were performed in the dark or under dim red light conditions ($\lambda > 630$ nm). Next, 11-*cis*-retinal was added as a freshly prepared concentrated solution in dimethylformamide to a final concentration of 40 μM and the entire mixture was incubated for at least 60 min under an argon atmosphere with constant rotation at ambient temperature. Occasionally, an additional overnight incubation at 4 °C was used.

Purification and reconstitution of recombinant rhodopsin

To the membranes containing the regenerated rhodopsin were added DOM (unless indicated otherwise) and 2-mercaptoethanol to final concentrations of 40 and 5 mM respectively. After incubation for at least 2 h at 4 °C with constant rotation under an argon atmosphere, the unsolubilized proteins were removed by centrifugation for 20 min at 80 000 *g* (4 °C). The concentration of rhodopsin in the supernatant was determined by UV/visible spectroscopy (see below). The supernatant was then adjusted to pH 7.0; NaCl and glycerol were added to 0.5 M and 20% (v/v) respectively. After centrifugation for 30 min at 100 000 *g* (4 °C), the supernatant was applied to a superflow Ni²⁺-nitrilotriacetic acid (NTA) column (Qiagen, Hilden, Germany) equilibrated in buffer A [20 mM Bis-Tris propane/Na⁺ (pH 7.0)/500 mM NaCl/10 mM KCl/3 mM MgCl₂/2 mM CaCl₂/0.1 mM EDTA/5 μM leupeptin/20% (v/v) glycerol/20 mM nonylglucoside/5 mM 2-mercaptoethanol]. The column was washed with 10 vol. of buffer A followed by 10 vol. of a linear gradient of buffer B in buffer A (buffer B was buffer A containing 5 mM histidine). Rhodopsin was eluted with buffer C (buffer A with 50 mM histidine and only 130 mM NaCl). Fractions containing rhodopsin were identified by UV/visible spectroscopy, monitoring the presence of its typical absorbance band with a maximum near 500 nm in unbleached samples. Rhodopsin containing fractions were pooled and the rhodopsin was reconstituted into a native bovine retina lipid environment at a molar lipid-to-protein ratio of 100:1 as described [13]. Reconstituted rhodopsin was separated from non-reconstituted material by sucrose-density-gradient centrifugation as described [13]. The sucrose in the resulting rhodopsin proteoliposome fraction was removed by repeated washing of the membranes with ultrapure water and subsequent centrifugation for 30 min at 80 000 *g* (4 °C). Membranes were stored as a pellet under an argon atmosphere at -80 °C.

UV/visible spectroscopy

Spectra were recorded from 250 to 700 nm on a Lambda-15 spectrophotometer (Perkin–Elmer, Norwalk, CT, U.S.A.). The

concentration of rhodopsin was determined from the difference in absorption at 498 nm in the presence of 50 mM hydroxylamine before and after photobleaching for 5 min by using a 100 W tungsten light bulb equipped with a 430 nm cut-off filter (Schott, Menden, Germany). The molar absorption coefficient at 498 nm was taken as 40 500 M⁻¹·cm⁻¹.

G-protein activation assay

Activation of the G-protein transducin was determined by using the fluorometric procedure described previously [14] on a Shimadzu RF-5301 spectrofluorometer with excitation at 295 nm and emission at 337 nm. In brief, a bleached rhodopsin sample (10 pmol) was added to a stirred cuvette containing 2 ml of 20 mM Hepes, pH 7.4, 100 mM NaCl, 2 mM MgCl₂, 1 mM dithioerythritol, 0.01% (w/v) DOM and 100 nM transducin. After the fluorescence emission signal had stabilized, guanosine 5'-[γ-thio]triphosphate (GTP[S]; Boehringer, Mannheim, Germany) was added to a final concentration of 2.5 μM and the activation of transducin was measured by means of the increase in intrinsic fluorescence of a tryptophan residue. Transducin activation assays were performed at 23 and 11 °C.

FTIR spectroscopy

FTIR spectra were recorded on a Bio-Rad FTS60a (Digilab Division, Cambridge, MA, U.S.A.), essentially as described previously [15].

RESULTS AND DISCUSSION

Optimization of rhodopsin expression

Culture medium

Two major factors that determine the volumetric yield of recombinant protein are the maximal obtainable cell density and the yield of recombinant protein per cell. Both of these parameters are likely to be influenced by the composition of the culture medium. Previously we used the serum-supplemented TNM-FH medium [16] for our insect cell culture. However, for both practical (see below) and economic reasons, we decided to switch to serum- and protein-free culture media. We therefore tested several commercially available serum-free insect cell growth media [Sf900II (Gibco-BRL, Rockville, MD, U.S.A.), EXCELL-400 and -401 (JRH Biosciences, Lenexa, KS, U.S.A.) and Insect-Xpress (BioWhittaker, Walkersville, MD, U.S.A.)] for their performance with regard to Sf9 cell growth rates, maximal cell densities and cellular expression level of recombinant rhodopsin. Sf9 cells were first gradually adapted to these serum-free media in monolayer culture. This was established by repeated serial passages in medium that was replaced with 25%, 50%, 75%, 95% and finally 100% serum-free medium, respectively. Cells were then transferred to spinner flasks and adapted to suspension culture. In our hands, the best results were obtained with Insect-Xpress. Cells fully adapted to Insect-Xpress medium had a doubling time of approx. 24 h, compared with 18 h in TNM-FH medium, and could reach densities of (7–9) × 10⁶/ml, compared with a maximum of 4 × 10⁶/ml in TNM-FH medium. However, these high cell densities were reached only with cells freshly adapted to Insect-Xpress medium. Subsequently, the maximum cell density decreased gradually to approx. (5–6) × 10⁶/ml over a period of approx. 2 months but then remained stable for at least 6 months. Recombinant rhodopsin production levels were also evaluated. Interestingly, under similar infection conditions the functional rhodopsin level obtained per cell in all serum-free insect cell culture media tested varied between at least equal to

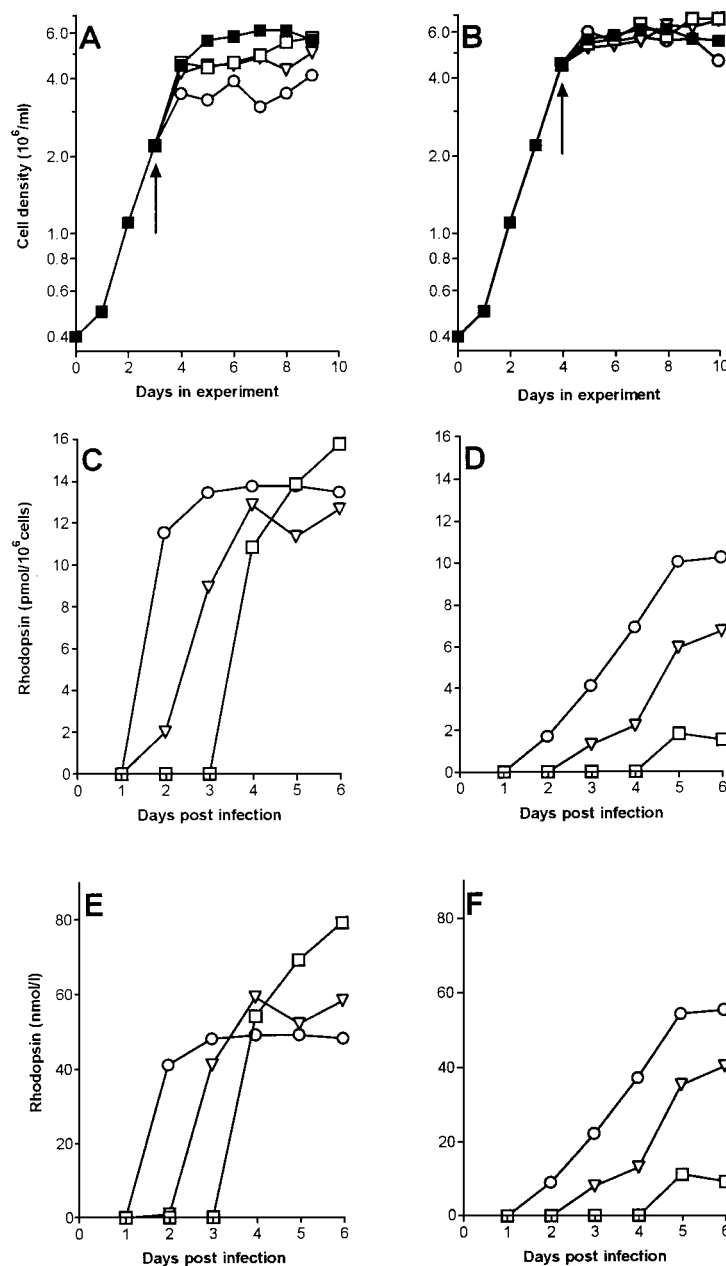


Figure 1 Production of hexahistidine-tagged rhodopsin in spinner flasks

Spinner cultures (100 ml) were infected in their mid-exponential phase of growth (A, C, E) or in the late-exponential phase of growth (B, D, F) at the following MOI values: ■, 0 (uninfected); □, 0.01; ▽, 0.1; ○, 1.0. The total cell densities (A, B), cellular rhodopsin yields (C, D) and volumetric rhodopsin yields (E, F) were monitored for up to 6 days after infection. The arrow in (A) and (B) indicates the time of infection. The results are typical of at least three similar experiments. To compensate for errors made in cell counts (typically approx. 10%), the cellular production levels were calculated by dividing the volumetric production levels by the average of the cell counts over days 2–6 after infection.

and up to double that reached in the serum-supplemented TNM-FH medium (results not shown). Because of the high cell density and the good cellular production levels, ultimately yielding maximal volumetric production levels, we decided to use Insect-Xpress medium for all subsequent expression studies.

Cell density and multiplicity of infection (MOI)

A number of factors influencing the yield of recombinant protein in the baculovirus expression system had already been examined. In these studies, special attention was given to the density at

which cells were infected and the amount of virus used for infection of the cells [17–19]. Most of this work focused on soluble cytosolic proteins such as β -galactosidase. However, it must be realized that high level expression of integral membrane proteins and secreted proteins will severely challenge the cell's secretory route (e.g. endoplasmic reticulum or Golgi). Processes such as membrane translocation, folding, N-glycosylation and palmitoylation probably determine the rate of recombinant protein production and hence affect expression levels. Therefore established conditions maximizing the production of soluble protein might not also be optimal for the production of membrane

protein. We therefore decided to establish optimal conditions for infection with regard to cell density and virus-to-cell ratio (MOI) for rhodopsin.

Commonly, infection of Sf9 cells is performed in the early exponential phase of growth at high MOI (at least 10) to ensure a synchronous infective process throughout the entire culture. However, because earlier analyses had already indicated that the effect of raising the MOI from 1 to 10 does not have a marked effect on the production level of recombinant rhodopsin [20], we examined only relatively low MOI ranges (0.01–1.0). These experiments were first done in small-scale suspension cultures (100 ml in spinner flasks) for cells in their early–mid-exponential and late-exponential phases of growth. The total cell numbers, cellular production yields and volumetric production yields were monitored for up to 6 days after infection. The result of a representative experiment is shown in Figure 1. When cells were infected in their early–mid-exponential phase of growth, their maximal recombinant rhodopsin production level was relatively unaffected by the MOI (Figure 1C). However, there was a clear difference in the onset of rhodopsin production. With an MOI of 1, rhodopsin production was first detected at approx. 2 days after infection and reached a maximum at approx. 3–4 days after infection. At MOI values below 1 the average onset of rhodopsin synthesis was delayed because it took some time for the initial infection to spread throughout the entire culture. During this period, uninfected cells were still able to divide, resulting in higher total cell counts (Figure 1A). This clearly also benefitted the volumetric yield of recombinant rhodopsin because larger numbers of cells could contribute to the production process. Therefore, when cells were infected in the early–mid-exponential phase of growth, the highest levels of recombinant rhodopsin production per culture volume were obtained with the lowest MOI value (0.01; Figure 1E).

When cells were infected in the late-exponential phase of growth, a completely different picture was obtained (Figures 1B, 1D and 1F): the amount of rhodopsin produced was strongly affected by the MOI, the highest levels being obtained with the highest MOI values. Also, the maximal cellular production levels did not reach the same level as for cells infected in their early–mid-exponential phase of growth. Finally, the additional advantage in volumetric yield when cells in the early–mid-exponential phase of growth were infected at low MOI (owing to the increase in total cell density) no longer prevailed, because all cultures reached the same approximate maximum cell density independently of the applied MOI.

Highest volumetric yields were obtained when cells in their early–mid-exponential phase of growth were infected with an MOI of 0.01. Cellular production levels reached approximately the same levels independently of the amount of virus used to infect the cells. This probably indicates that there is a maximum amount of recombinant membrane protein that a single cell can accommodate and that this level can be reached as long as the cells remain viable. However, with a lower MOI uninfected cells are still able to divide, thereby increasing the total number of cells ultimately included in the production process. This will of course only occur if cell growth itself is not compromised, i.e. if the growth medium contains enough nutrients and there is no significant build-up of waste products that might inhibit cell growth. Therefore the culture must be infected in an early phase of growth. If nutrient availability is compromised or if there is an accumulation of waste products (e.g. in a culture that is infected at the late-exponential phase of growth), the total infective process is apparently severely hampered. Our results demonstrate that this affects functional production levels of a recombinant membrane protein.

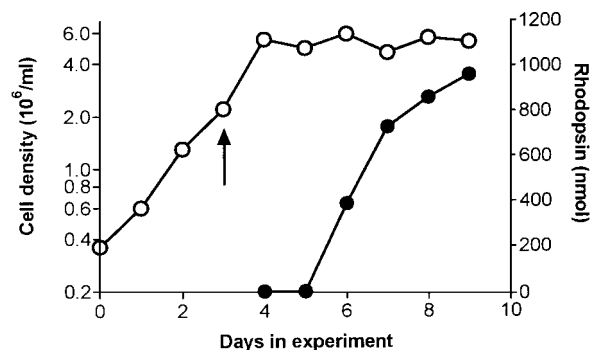


Figure 2 Production of hexahistidine-tagged rhodopsin in a bioreactor

A 10-litre bioreactor culture was infected at 2.2×10^6 cells/ml with an MOI of 0.01. The total cell density (○) and the total amount of rhodopsin produced (●) were monitored for up to 6 days after infection. The arrow indicates the time of infection. Results are representative of several similar experiments.

Large-scale culture

Conditions yielding optimal volumetric production of rhodopsin in small-scale cultures were then applied to a large-scale (10-litre) bioreactor culture (infection of a mid-exponential-phase culture at an MOI of 0.01). A representative experiment is shown in Figure 2. The results for the aerated 10-litre vessel were almost identical to those for the 100 ml spinner cultures, ultimately yielding close to $1 \mu\text{mol}$ (approx. 40 mg) of rhodopsin in one batch. This was unexpected, because scaling up of a biological system is usually accompanied by a loss of productivity. Initially, we tried to scale up the expression volumes by using spinner flasks with larger working volumes (up to 1 litre). However, without active aeration in the flasks, both cell growth parameters and recombinant protein yield were negatively affected (G. L. J. DeCaluwé, P. M. A. M. Vissers and W. J. DeGrip, unpublished work). This indicates that the Sf9 cells have a relatively large oxygen demand. Whereas the culture conditions in a spinner flask are more or less a black box, the partial oxygen pressure in the 10-litre bioreactor culture is constantly monitored and adjusted when necessary. Therefore any compromise in recombinant protein yield because of the larger scale will largely be compensated for by the more stable and better controlled culture conditions.

The ability to apply low MOI values to large-scale bioreactor cultures has a clear advantage over high MOI values because a much smaller viral inoculum is required. For instance, infection of a 10-litre culture at 2×10^6 cells/ml with an MOI of 10 would require 2 litres of high-titre viral inoculum (typically 10^8 plaque-forming units/ml). Our results show that the amount of virus can be decreased by a factor of 1000 without compromising total recombinant protein yield. Therefore a viral stock obtained from a standard-sized culture flask (75 cm², or 10 ml of culture) will usually yield enough viruses to infect several 10-litre bioreactor cultures with an MOI of 0.01.

Optimization of rhodopsin purification

C-terminal compared with N-terminal hexahistidine tag

We had demonstrated previously on small batches that extending rhodopsin with a hexahistidine tag allowed the rapid single-step purification of recombinant rhodopsin with immobilized-metal-affinity chromatography [12]. We also examined the potential of an N-terminally placed hexahistidine tag. This construct express-

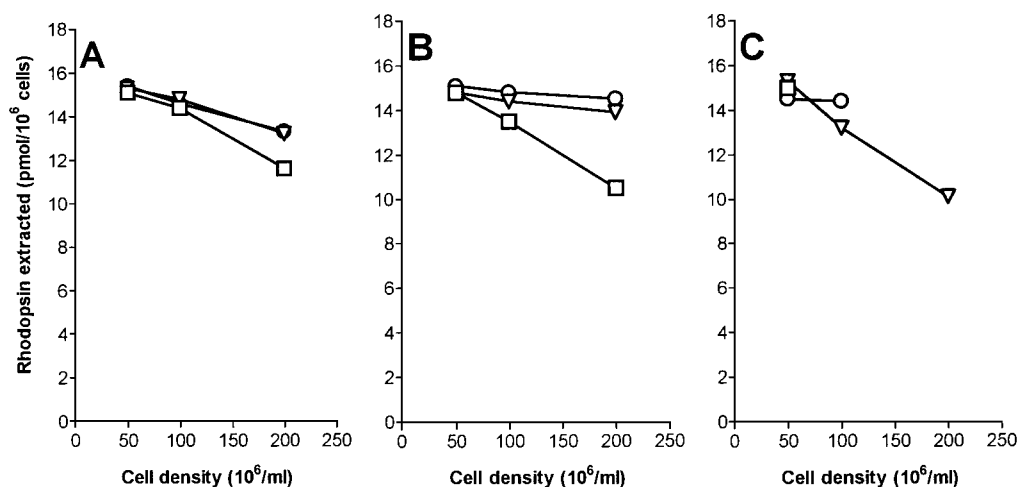


Figure 3 Extraction of recombinant hexahistidine-tagged rhodopsin from Sf9 cell membranes

Sf9 membranes containing recombinant histidine-tagged rhodopsin were prepared as described in the text and incubated at several concentrations (corresponding to the equivalent number of cells/ml) with DOM (A), CHAPS (B) or NG (C) at 20 mM (□), 40 mM (▽) or 60 mM (○), for at least 2 h at 4 °C under constant rotation. After the removal of non-solubilized material by centrifugation, the amount of rhodopsin in the supernatant was determined by UV/visible spectroscopy and expressed as pmol of rhodopsin per 10⁶ cells. The absence of several data points in the NG graph was caused by the turbidity of the samples after the standard centrifugation procedure, making it impossible to determine the rhodopsin concentration accurately.

ed functional rhodopsin at similar levels to those of its C-terminal counterpart. However, we could not find any condition under which N-terminal His-tagged rhodopsin would bind with sufficient affinity to the immobilized-metal columns to allow reasonable purification (results not shown). Possibly the His-tag is not sufficiently accessible or is too structurally restrained to complex with the matrix-bound metal ion. Because it is difficult to predict what effect the insertion of additional amino acid residues between the rhodopsin N-terminus and the His-tag would have on the topologically rather sensitive intraluminal domain of rhodopsin, we abandoned the N-terminal His-tag approach. Instead, we optimized the extraction and purification of C-terminally His-tagged rhodopsin to achieve optimal recoveries for large batches (up to 5 mg of rhodopsin).

Detergent solubilization and affinity purification of His-tagged rhodopsin

For large-scale production it is particularly important to find optimal conditions for the solubilization and purification of a membrane protein, to minimize working volumes, to make procedures as efficient as possible and to maximize recovery. Much effort was put into finding the most suitable detergent(s) to solubilize recombinant rhodopsin from the insect cell membranes for subsequent binding to the metal-affinity matrix. Crude membrane fractions from infected Sf9 cells were incubated at several densities with DOM, NG or CHAPS at various concentrations for at least 2 h at 4 °C. These detergents were selected because they represent different classes of detergent and maintain a relatively high thermal stability of rhodopsin [21]. This is important for optimal recovery, particularly for processing rhodopsin mutants, which often show a decrease in thermal stability. After the precipitation of unsolubilized material, the concentration of rhodopsin in the supernatant was determined (Figure 3). At membrane suspensions of a relatively low concentration (equivalent to 5×10^7 cells/ml) moderate concentrations of detergent (20 mM) allow the quantitative extraction of rhodopsin. However, for large-scale purification procedures, the extraction volume is an important parameter because it determines for example the quantity of chemicals required and the

time needed for centrifugation and column loading. At 4-fold more concentrated membrane suspensions (equivalent to up to 2×10^8 cells/ml), most of the rhodopsin could still be extracted but now required higher detergent concentrations. Yields of more than 80% or more than 90% were achievable with at least 40 mM DOM or CHAPS respectively. NG performed less well at more concentrated membrane suspensions, even at elevated concentrations. NG extracts obtained from such membrane suspensions were often very turbid, requiring additional prolonged ultracentrifugation steps to determine the rhodopsin concentration accurately. Even then, the extracts proved highly unstable unless extreme care was taken to avoid temperature fluctuations.

In addition to the ability of a detergent to extract rhodopsin from the insect cell membranes, another important parameter is the ability to allow quantitative binding of the solubilized recombinant rhodopsin to the Ni²⁺-agarose matrix. No elaborate efforts were made to distinguish between the various available immobilized-metal-affinity chromatography matrices. However, in several small-scale trials, superflow Ni²⁺-NTA-agarose (Qiagen) emerged as the optimal matrix for C-terminally hexahistidine-tagged rhodopsin. We tested the binding capacity of the Ni²⁺-NTA matrix for the hexahistidine-tagged rhodopsin solubilized with either DOM or CHAPS (Figure 4). This was done in batches by varying the amount of matrix added per ml of extract. In both cases, more than 90% of the solubilized rhodopsin could be cleared from the extract after incubation with saturating amounts of matrix suspension (at least 40 μl/ml). However, when the amount of matrix was limited, CHAPS-solubilized rhodopsin was cleared from the extract much more efficiently than DOM-solubilized rhodopsin. From these results it can be calculated that the binding capacity of the Ni²⁺ matrix is approx. 40–50 nmol/ml of matrix for rhodopsin solubilized in DOM, compared with 70–80 nmol/ml for rhodopsin solubilized in CHAPS.

Affinity-immobilized rhodopsin could be eluted quantitatively with a histidine gradient. Previously we used a step gradient of imidazole to remove low-affinity contaminants, finally eluting rhodopsin with 200 mM imidazole [12]. This high concentration

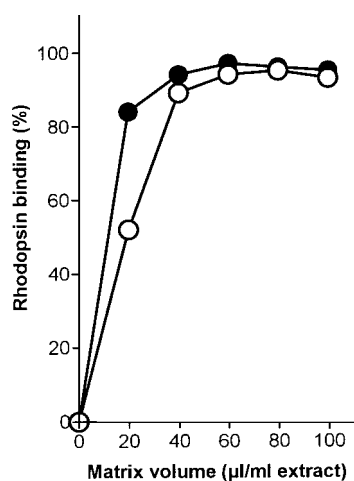


Figure 4 Binding of hexahistidine-tagged rhodopsin to the Ni^{2+} -agarose affinity matrix

Recombinant histidine-tagged rhodopsin was extracted from Sf9 membranes suspended at a concentration equivalent to 2×10^8 cells/ml with either 40 mM DOM (○) or 40 mM CHAPS (●). The solutions were adjusted to pH 7.0, made 20% (v/v) in glycerol and 0.5 M in NaCl, and incubated with various amounts of Ni^{2+} -NTA agarose for 16 h under constant rotation. The matrix was pelleted by centrifugation for 1 min at 1000 g and the amount of rhodopsin cleared from the supernatant was determined by UV/visible spectroscopy. Initial rhodopsin concentrations were 1.8 nmol/ml for DOM and 1.7 nmol/ml for CHAPS.

of imidazole can destabilize visual pigments (P. H. M. Bovee-Geurts, P. M. A. M. Vissers and W. J. DeGrip, unpublished work), so we examined whether histidine would be a satisfactory

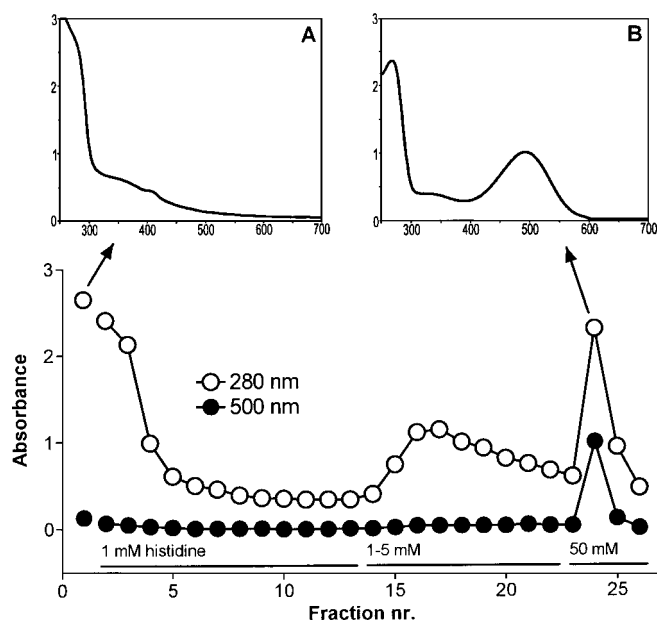


Figure 5 Single-step purification of hexahistidine-tagged rhodopsin

A typical elution profile is shown for C-terminally hexahistidine-tagged rhodopsin bound to Ni^{2+} -NTA agarose with the use of histidine as eluent. A total of 70 nmol of rhodopsin was absorbed on 2 ml of matrix; fractions of approx. 2 ml were collected. See the Materials and methods section for further details. Inset A: UV/visible spectrum of the total membrane extract loaded on the column. Inset B: UV/visible spectrum of the major fraction, eluted with 50 mM histidine. The units of the y-axes and x-axes of the insets are absorbance and nm respectively.

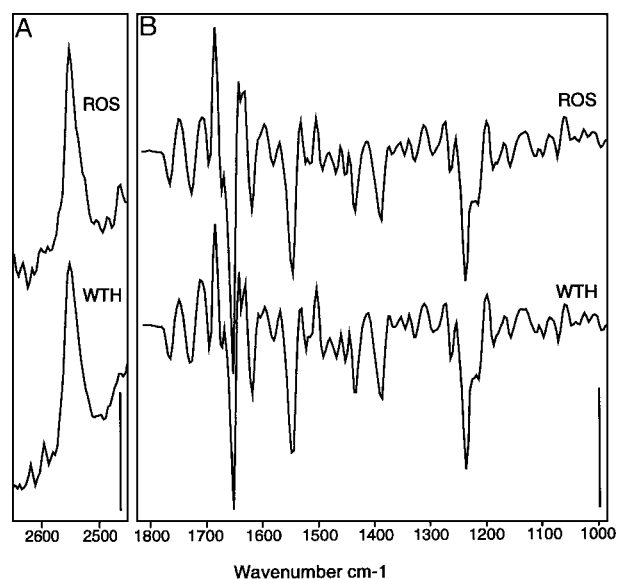


Figure 6 FTIR analysis of native rhodopsin and recombinant hexahistidine-tagged recombinant rhodopsin

FTIR difference spectra are shown for the transition from the dark state to the metarhodopsin II intermediate in both bovine native rhodopsin from rod outer segments (ROS) and bovine recombinant wild-type histidine-tagged rhodopsin (WTH). The spectral regions shown are those in which some of the major changes in vibrational activity occur, e.g. 1800–1000 cm^{-1} [protein and chromophore fingerprint region (B)] and 2600–2500 cm^{-1} [-SH vibrations (A)]. Scale bar, 5×10^{-3} absorbance units in (B) and 0.2×10^{-3} absorbance units in (A).

alternative. Indeed, lower concentrations of histidine (30–50 mM) afforded maximal elution of bound rhodopsin. A typical elution profile is shown in Figure 5. The eluted peak fractions commonly contained at least 80% of the bound rhodopsin with A_{280}/A_{500} in the range 2.0–2.3, showing the typical UV/visible absorbance profile of rhodopsin (Figure 5, inset B). Reconstitution of the purified solubilized rhodopsin into a native-like lipid environment (retina lipids) was established by selective extraction of detergent with β -cyclodextrin, after the addition of retina lipids in a molar ratio to rhodopsin of 100:1. Subsequent sucrose-density-gradient centrifugation separated proteoliposomes from non-reconstituted material. The reconstitution was performed essentially in accordance with the protocol reported previously [13], with a recovery of approx. 80%. Reconstitution simultaneously affords further purification, yielding rhodopsin preparations with A_{280}/A_{500} of 1.7–1.8, indicating purities better than 95%.

Functional characteristics of recombinant His-tagged rhodopsin

After production and purification as described above, the recombinant His-tagged rhodopsin was functionally characterized. As shown in Figure 5 (inset B), the UV/visible spectral characteristics of unbleached samples closely corresponded to those of the native protein. Previously we had reported that His-tagging induces a subtle red-shift (2–3 nm) of the absorbance spectrum of rhodopsin [12]. Since then we have analysed a large number of preparations. Larger batches, which allow more precise analysis, exhibit spectral properties ($\lambda_{\text{max}} 498 \pm 2$ nm) identical to those of native rhodopsin. However, the slight down-shift in the pK_a of the meta I/meta II equilibrium in His-tagged rhodopsin (approx. 0.2 pH units), also reported previously [12], was reproducibly observed. Because the pK_a depends strongly on the surface

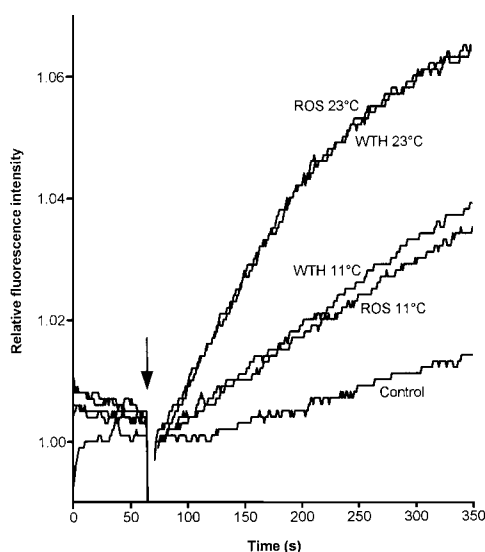


Figure 7 G-protein activation assay of native rhodopsin and recombinant hexahistidine-tagged rhodopsin

Activation of the G-protein transducin by either native bovine rhodopsin from rod outer segments (ROS) or bovine recombinant wild-type histidine-tagged rhodopsin (WTH), assayed by the increase of G α tryptophan fluorescence on binding of GTP. Rhodopsin (10 pmol) was mixed with a 20-fold excess of transducin and illuminated. After stabilization of the fluorescence emission intensity (λ_{ex} 295 nm, λ_{em} 337 nm), GTP[S] was added to a final concentration of 2.5 μ M (arrow). The rate of the subsequent increase in emission intensity represents the capacity of rhodopsin to activate transducin. The assay was performed at 23 and 11 $^{\circ}$ C. Note that there is no significant difference between the rates generated by native or recombinant His-tagged rhodopsin at either temperature. The control curve was obtained at 23 $^{\circ}$ C without the addition of either photopigment.

charge [22], this effect might be caused by the slight additional positive charge contributed by the histidine residues.

However, spectral characteristics are only a global indication that the recombinant rhodopsin is structurally identical with the native protein. We therefore applied a more comprehensive technique, FTIR difference spectroscopy, to study the protein conformational changes accompanying photoactivation of recombinant His-tagged rhodopsin. In Figure 6, FTIR difference spectra are shown for the transition from rhodopsin to metarhodopsin II. These difference spectra are the net result of the changes in infrared-sensitive vibrations that occur between the rhodopsin dark state and the metarhodopsin II photo-intermediate state. Close examination shows that these difference spectra have exactly the same band profile for both His-tagged and native rhodopsin. The same result was obtained for earlier intermediates (bathorhodopsin, lumirhodopsin and metarhodopsin I; results not shown). Therefore the recombinant protein proceeds through exactly the same structural transitions. This presents unequivocal evidence that the structures of the native and recombinant proteins are identical.

Because the metarhodopsin II intermediate is the active intermediate, these findings also strongly suggest that the 'recombinant' metarhodopsin II should retain the full potential to bind and activate the G-protein transducin. This functional property was studied with an assay based on the change of intrinsic tryptophan fluorescence on the binding of GTP[S] to the G α subunit. In Figure 7, the results of this assay are shown for both native and His-tagged recombinant rhodopsin. Clearly, the recombinant rhodopsin is indeed capable of binding and activating its G-protein transducin. Furthermore, the kinetics at 23

and 11 $^{\circ}$ C are indistinguishable for the native and recombinant proteins. Results from several similar experiments yielded an activity for recombinant rhodopsin of $102 \pm 6\%$ ($n = 6$) relative to the native protein, demonstrating that the recombinant protein retains full activity. Evidently, the His-tag and the small amount of additional positive charge that it carries [22] perturb neither the structural transitions in the photoactivation cascade nor the interaction with the G-protein transducin.

Implications for other membrane proteins

We have provided a framework that can be followed to optimize the expression and purification of functional recombinant membrane proteins by using the baculovirus expression system as exemplified for bovine hexahistidine-tagged rhodopsin, a member of the G-protein-coupled receptor family. For the expression of rhodopsin, this system performs very well, reaching expression levels of $(1.0\text{--}1.5) \times 10^7$ functional copies per cell, which is a major improvement over other expression systems. The maximal expression level that we have observed for rhodopsin is approx. 30 pmol/ 10^6 cells (approx. 1.8×10^7 copies per cell). We are quite confident that in principle similar expression levels can be achieved in this system with any other membrane protein. It is of course crucial to determine the percentage of the expressed protein that is fully functional. For rhodopsin this situation is quite favourable, ranging from 60% to 80% functional protein [20]. However, this might vary considerably for other proteins, owing to intrinsic and/or extrinsic factors. On the one hand, mutations might intrinsically decrease the folding rate and/or the thermal stability of a membrane protein, thereby challenging the quality control resources of the endoplasmic reticulum and the degradative capacity of the cell. Such effects cannot be solved by switching to another expression system, and in fact will generate similar problems in the native tissue. Indeed, a large number of rhodopsin mutants have been identified that remain largely in the endoplasmic reticulum after heterologous expression; *in vivo* they may even evoke slow degeneration of the photoreceptor cell [23]. High-level functional expression of such mutant receptors will require special measures, such as increasing the capacity of the endoplasmic reticulum or decreasing the culture temperature.

On the other hand, native proteins might also show low functionality after heterologous expression. For instance, with the conditions optimized for rhodopsin we could also achieve high protein expression levels in the baculovirus system for several other G-protein-coupled receptors, namely the red and green cone visual pigments [14,24] and the histamine H1 and H2 receptors ([25], and H. G. P. Swarts, J. VanOostrum, C. H. W. Klaassen, R. Leurs and W. J. DeGrip, unpublished work). However, the level of functional protein varied considerably from 10–20% for the H2 receptor, 20–40% for the red cone pigment to 40–60% for the green cone pigment and the H1 receptor. Immunochemical studies showed that a large part of the expressed protein is indeed not glycosylated and still resides in the endoplasmic reticulum. Because the folding and/or the stabilization of proteins sometimes depend on specific factors in the native tissue [26,27], identification and co-expression might be one, albeit tedious, way of addressing this problem. A more general solution, such as a significant increase in the quality control capacity of the endoplasmic reticulum, would be preferable. These approaches are currently under investigation. Interestingly, we observed that expression in the bioreactor invariably yielded the highest level of functionality, suggesting that a carefully controlled culture environment would make a

general contribution to optimizing functional heterologous expression.

We also report procedures for the optimal solubilization and affinity purification of recombinant hexahistidine-tagged rhodopsin. However, these results cannot be directly extrapolated to other membrane proteins because solubilization of the proteins with the purpose of maintaining them in a sufficiently stable state to survive purification depends partly on very specific protein–lipid and protein–detergent interactions. For instance, whereas detergents such as DOM or CHAPS perform rather well for many membrane proteins, often agents such as glycerol, lipids or salts [14,28–30] have to be added to achieve better solubilization and/or to maintain sufficient stability. Occasionally even special detergents have been shown to be required [31,32]. Solubilizing conditions can therefore be taken from a general principle, such as that shown for rhodopsin, but need to be optimized for each protein.

In conclusion, our approach outlined here presents a general framework for optimizing the expression and purification of eukaryotic membrane proteins on a scale that would allow subsequent biophysical studies into their structure and mechanism.

We thank Dr. Rosalie Crouch for her gift of 11-*cis*-retinal and Dr. Kenneth J. Rothschild for his co-operation on the FTIR experiments. Part of this work was supported by a grant from the European Community (BIO2-CT93-0467) to W.J.D.G.

REFERENCES

- Hargrave, P. A. and McDowell, J. H. (1992) *Int. Rev. Cytol.* **137B**, 49–97
- Franke, R. R., König, B., Sakmar, T. P., Khorana, H. G. and Hofmann, K. P. (1990) *Science* **250**, 123–125
- DeCaluwé, G. L. J., Bovee-Geurts, P. H. M., Rath, P., Rothschild, K. J. and DeGrip, W. J. (1995) *Biophys. Chem.* **56**, 79–87
- DeCaluwé, G. L. J. and DeGrip, W. J. (1996) *Biochem. J.* **320**, 807–815
- Han, M., Lin, S. W., Smith, S. O. and Sakmar, T. P. (1996) *J. Biol. Chem.* **271**, 32330–32336
- Han, M., Smith, S. O. and Sakmar, T. P. (1998) *Biochemistry* **37**, 8253–8261
- Gröbner, G., Choi, G., Burnett, I. J., Glaubitz, C., Verdegem, P. J. E., Lugtenburg, J. and Watts, A. (1998) *FEBS Lett.* **422**, 201–204
- Ujj, L., Jäger, F. and Atkinson, G. H. (1998) *Biophys. J.* **74**, 1492–1501
- Oprian, D. D., Molday, R. S., Kaufman, R. J. and Khorana, H. G. (1987) *Proc. Natl. Acad. Sci. U.S.A.* **84**, 8874–8878
- Mollaaghababa, R., Davidson, F. F., Kaiser, C. and Khorana, H. G. (1996) *Proc. Natl. Acad. Sci. U.S.A.* **93**, 11482–11486
- Reeves, P. J., Thurmond, R. L. and Khorana, H. G. (1996) *Proc. Natl. Acad. Sci. U.S.A.* **93**, 11487–11492
- Janssen, J. J. M., Bovee-Geurts, P. H. M., Merckx, M. and DeGrip, W. J. (1995) *J. Biol. Chem.* **270**, 11222–11229
- DeGrip, W. J., VanOostrum, J. and Bovee-Geurts, P. H. M. (1998) *Biochem. J.* **330**, 667–674
- Vissers, P. M. A. M., Bovee-Geurts, P. H. M., Portier, M. D., Klaassen, C. H. W. and DeGrip, W. J. (1998) *Biochem. J.* **330**, 1201–1208
- DeLange, F., Klaassen, C. H. W., Wallace-Williams, S. E., Bovee-Geurts, P. H. M., Liu, X., DeGrip, W. J. and Rothschild, K. J. (1998) *J. Biol. Chem.* **273**, 23735–23739
- Summers, M. D. and Smith, G. E. (1987) *Texas Exp. Station Bull.* no. 1555
- Licari, P. J. and Bailey, J. E. (1992) *Biotechnol. Bioeng.* **39**, 432–441
- Power, J. F., Reid, S., Radford, K. M., Greenfield, P. F. and Nielsen, L. K. (1994) *Biotechnol. Bioeng.* **44**, 710–719
- Wong, K. T. K., Peter, C. H., Greenfield, P. F., Reid, S. and Nielsen, L. K. (1996) *Biotechnol. Bioeng.* **49**, 659–666
- DeCaluwé, G. L. J., VanOostrum, J., Janssen, J. J. M. and DeGrip, W. J. (1993) *Methods Neurosci.* **15**, 307–321
- DeGrip, W. J. (1982) *Methods Enzymol.* **81**, 256–265
- DeLange, F., Merckx, M., Bovee-Geurts, P. H. M., Pistorius, A. M. A. and DeGrip, W. J. (1997) *Eur. J. Biochem.* **243**, 174–180
- Gal, A., Apfelstedt-Sylla, E., Janecke, A. R. and Zrenner, E. (1997) *Prog. Retin. Eye Res.* **16**, 51–79
- Vissers, P. M. A. M. and DeGrip, W. J. (1996) *FEBS Lett.* **396**, 26–30
- Beukers, M. W., Klaassen, C. H. W., DeGrip, W. J., Verzijl, D., Timmerman, H. and Leurs, R. (1997) *Br. J. Pharmacol.* **122**, 867–874
- Ferreira, P. A., Nakayama, T. A. and Travis, G. H. (1997) *Proc. Natl. Acad. Sci. U.S.A.* **94**, 1556–1561
- Gomez, S. and Morgans, C. W. (1993) *J. Biol. Chem.* **268**, 19593–19597
- Keinänen, K., Köhr, G., Seeburg, P. H., Laukkanen, M. and Oker-Blom, C. (1994) *Bio/Technology* **12**, 802–806
- VonJagow, G., Link, T. A. and Schägger, H. (1994) in *A Practical Guide to Membrane Protein Purification* (VonJagow, G. and Schägger, H., eds.), pp. 3–21, Academic Press, San Diego
- Vuillard, L., Braun-Breton, C. and Rabilloud, T. (1995) *Biochem. J.* **305**, 337–343
- Kessi, J., Poirée, J.-C., Wehrli, E., Bachofen, R., Semenza, G. and Hauser, H. (1994) *Biochemistry* **33**, 10825–10836
- Ramjeesingh, M., Li, C. H., Garami, E., Huan, L., Hewryk, M., Wang, Y. C., Galley, K. and Bear, C. E. (1997) *Biochem. J.* **327**, 17–21

Received 11 March 1999/21 May 1999; accepted 11 June 1999